LETTER

doi:10.1038/nature09513

Pericytes are required for blood–brain barrier integrity during embryogenesis

Richard Daneman[1], Lu Zhou[2], Amanuel A. Kebede[1] & Ben A. Barres[2]

Vascular endothelial cells in the central nervous system (CNS) form a barrier that restricts the movement of molecules and ions between the blood and the brain. This blood–brain barrier (BBB) is crucial to ensure proper neuronal function and protect the CNS from injury and disease[1]. Transplantation studies have demonstrated that the BBB is not intrinsic to the endothelial cells, but is induced by interactions with the neural cells[2]. Owing to the close spatial relationship between astrocytes and endothelial cells, it has been hypothesized that astrocytes induce this critical barrier postnatally[3], but the timing of BBB formation has been controversial[4–9]. Here we demonstrate that the barrier is formed during embryogenesis as endothelial cells invade the CNS and pericytes are recruited to the nascent vessels, over a week before astrocyte generation. Analysing mice with null and hypomorphic alleles of *Pdgfrb*, which have defects in pericyte generation, we demonstrate that pericytes are necessary for the formation of the BBB, and that absolute pericyte coverage determines relative vascular permeability. We demonstrate that pericytes regulate functional aspects of the BBB, including the formation of tight junctions and vesicle trafficking in CNS endothelial cells. Pericytes do not induce BBB-specific gene expression in CNS endothelial cells, but inhibit the expression of molecules that increase vascular permeability and CNS immune cell infiltration. These data indicate that pericyte–endothelial cell interactions are critical to regulate the BBB during development, and disruption of these interactions may lead to BBB dysfunction and neuroinflammation during CNS injury and disease.

To understand the mechanisms of BBB formation, we investigated the sequence of cell generation and BBB formation in the developing CNS (Fig. 1 and Supplementary Figs 1–7). In the rat cerebral cortex, angiogenesis begins at embryonic day 12 (E12), as endothelial cells invade the neural tissue from the surrounding vascular plexus (Fig. 1a and Supplementary Fig. 1). Pericytes—platelet-derived growth factor receptor-β (PDGFR-β)$^{+}$NG2^{+} vascular support cells—are found associated with endothelial tubes as nascent vessels are generated (Fig. 1b and Supplementary Fig. 1). Neural cells are produced from progenitors in a defined sequence, with neurons generated before glia. Oligodendroglia progenitor cells (OPCs), PDGFR-α^{+}NG2^{+} glial cells, are first observed at E19 and migrate throughout the cortex by birth (Fig. 1c). Astrocytes are first generated directly after birth and extend processes which contact vessels during the first postnatal week (Fig. 1d and Supplementary Fig. 2). If astrocytes induce the BBB, barrier properties should only be acquired after birth.

We next examined endothelial cell protein expression and barrier function during rat cortical development. BBB-forming endothelial cells are characterized by tight junctions, low rates of transcytosis, and the expression of specialized influx and efflux transporters. Tight junction molecules occludin, claudin 5 and ZO-1 were each expressed at endothelial junctions as early as E12 (Fig. 1e, Supplementary Fig. 4 and not shown). The same was observed with the BBB-specific influx transporter Glut1 (Fig. 1f and Supplementary Fig. 3). Notably, the BBB-specific efflux transporter Pgp is expressed at low levels during embryogenesis, but increases during postnatal development (Fig. 1g), indicating a distinct regulation mechanism for efflux transport. Similar timing of cell generation and BBB gene expression was observed in the developing mouse, with vascularization of the cortex starting at E11 (Supplementary Fig. 6). The expression of genes that increase vascular permeability, including transcytosis (*Plvap*) and leukocyte infiltration (*Icam1*), decreased after initial high expression (Supplementary Fig. 7). The developmental timing of BBB function was examined by trans-cardiac perfusion with tracers. In adults, the small molecule tracer biotin stays within the lumen of CNS vessels and doesn't diffuse into the CNS parenchyma, whereas in non-neural tissue the tracer diffuses throughout the extracellular space (Fig. 1h–j). We used this method to examine BBB function in postnatal animals and dissected embryos. At each age tested (E15, E21, P1, P15 and P20) CNS vessels excluded the tracer from the CNS parenchyma (Fig. 1h–j and not shown). In embryonic time points, the tracer was excluded from most of the CNS; however, distinct regions of the CNS displayed leakiness, including regions close to the pia (Supplementary Fig. 5), indicating that serum contents may enter the CNS through pial coverings or choroid plexus. Thus, a functional BBB is present during embryogenesis before astrocyte generation.

Because pericyte recruitment to CNS vessels temporally correlates with the onset of barrier properties, we examined the role of these mural cells in regulating BBB function, structure and gene expression. Although pericytes are associated with the vasculature throughout the body, and thus are unlikely candidates to regulate brain-specific vascular properties, recent studies have demonstrated that CNS pericytes have a different developmental origin from other pericytes[10], and several studies have suggested that pericytes are capable of regulating BBB properties *in vitro*[11–13]. To determine if pericytes are necessary for BBB formation we compared the vascular permeability of *Pdgfrb*$^{-/-}$ mice with littermate controls. PDGFBB signalling through PDGFR-β is essential for pericyte generation, and mice deficient for either the ligand or receptor completely lack CNS pericytes[14,15], exhibit endothelial cell hyperplasia, increased vessel diameter and morphological signs of increased vascular permeability[16]. These mice die at birth; therefore, we examined BBB function in dissected embryos. Indeed, *Pdgfrb*$^{-/-}$ mice show an increased vascular permeability to biotin (0.5 kDa), as observed by an increase in tracer staining throughout the CNS parenchyma (Fig. 2a, b). Decreasing permeability was observed with increasing size of tracer (Fig. 2c).

CNS vessels have the highest pericyte coverage of any vessels, and the extent of pericyte coverage in vessels throughout the body inversely correlates with the relative permeability of these vessels[17]. To determine whether pericyte number, and not just presence or absence, is an important regulator of BBB permeability, we measured CNS vascular permeability in mice with different combinations of null, hypomorphic and wild-type *Pdgfrb* alleles. One study[15] generated an allelic series of *Pdgfrb* hypomorphs, showing that varying the strength of PDGFR-β signalling leads to different pericyte:endothelial cell ratios. We compared the vascular permeability of *Pdgfrb*$^{F7/-}$ and *Pdgfrb*$^{F7/F7}$,

[1]UCSF Department of Anatomy, 513 Parnassus Avenue, HSW1301, San Francisco, California 94143-0452, USA. [2]Stanford University School of Medicine, Department of Neurobiology, Fairchild Science Building D200, Stanford, California 94305-5125, USA.

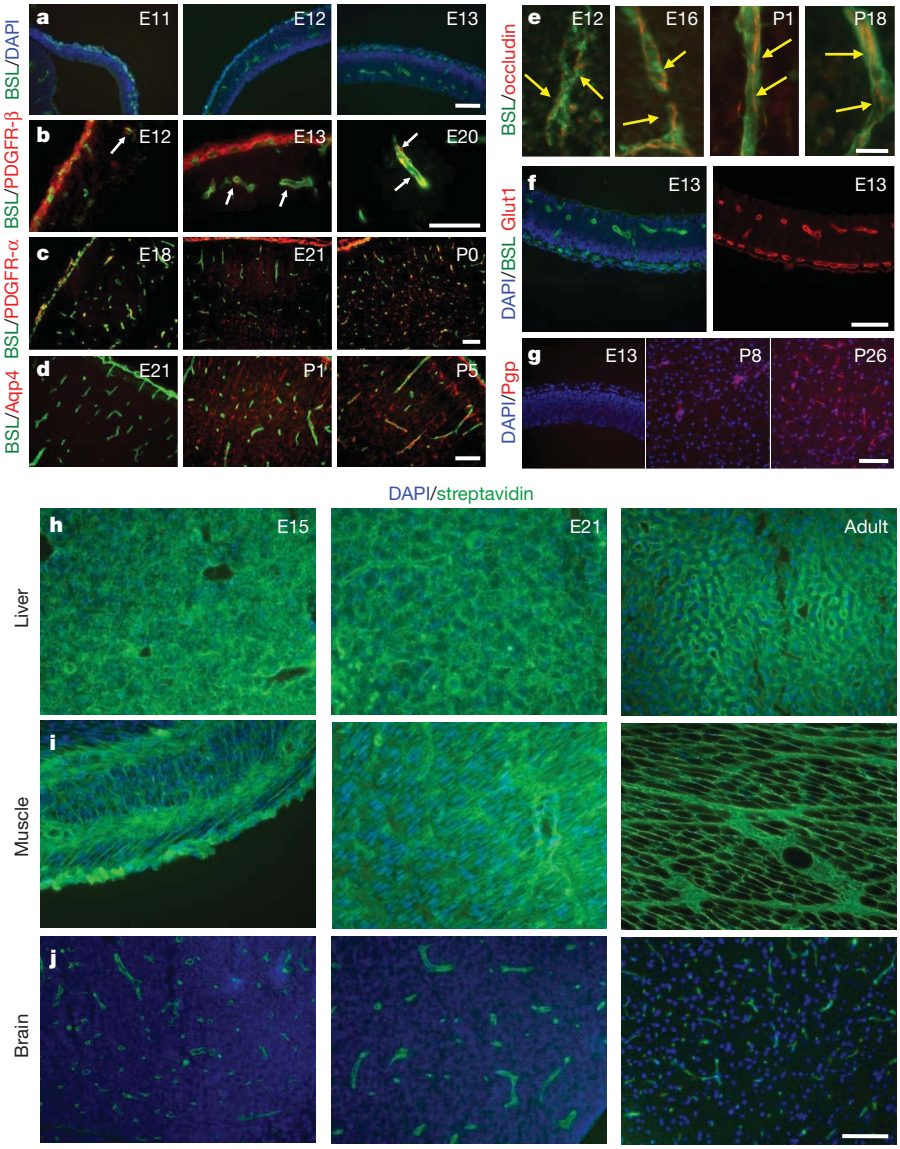

Figure 1 | Time course of cell generation and BBB development in the rat cerebral cortex. **a**–**g**, Sections of rat cerebral cortex at indicated ages were stained for endothelial cells with *Bandeiraea simplicifolia* lectin I (BSL) (green, **a**–**f**) and nuclei with DAPI (blue, **a**, **f** (left), **g**), pericytes with anti-PDGFR-β (red, **b**; white arrows point to pericytes), oligodendrocyte progenitors with anti-PDGFR-α (red, **c**), astrocytes with anti-aquaporin 4 (red, **d**), anti-occludin (red, **e**; yellow arrows indicate tight-junction strands), anti-Glut1 (red, **f** (right)), and anti-Pgp (red, **g**). Scale bars represent 100 μm (**a**–**d**, **f**, **g**) and 20 μm (**e**). **h**–**j**, Rats aged E15 (left), E21 (middle) and adults (right) were given a trans-cardiac perfusion of biotin, and liver (**h**), muscle (**i**) and brain (**j**) tissue sections were stained with streptavidin (green) and DAPI (blue). Scale bar represents 100 μm.

which respectively have approximately 40% and 50% of the pericyte coverage of littermate controls[15] (Fig. 2d–g and Supplementary Fig. 8). Indeed, the permeability of the BBB in these neonatal mice, to both Evan's blue and biotin, inversely correlated with the pericyte coverage (Fig. 2h–k), demonstrating that pericyte number determines relative permeability of CNS vessels during development.

We next addressed the question of whether pericytes regulate endothelial transcytosis, tight-junction formation and/or transporter expression. Examination by electron microscopy revealed that CNS endothelial cells of *Pdgfrb*$^{-/-}$ mice displayed an increase in membrane folding with membrane protrusions into the vessel lumen, as well as an increase in the number of cytoplasmic vesicles, indicating an increased rate of transcytosis (Fig. 3A–C). Indeed, examination of biotin leakage by electron microscopy, using streptavidin–horseradish peroxidise (HRP), revealed that the tracer was endocytosed into endothelial cell vesicles (Fig. 3A, d, e, and B, d, e), demonstrating transcellular passage is an important component of BBB leakiness in *Pdgfrb*$^{-/-}$ mice. *Pdgfrb*$^{-/-}$ mice and littermate controls expressed tight-junction proteins occludin and claudin 5 at equal levels and these molecules were localized to cellular junctions (Figs 3E, F and 4a, b). Structural abnormalities in the tight junctions of the *Pdgfrb*$^{-/-}$ mice were observed by electron microscopy (Fig. 3A, c and B, c). In control animals, the length of the junction was parallel to the plane of the vessel lumen; however, in *Pdgfrb*$^{-/-}$ mice, the junctional alignment was random, being parallel, perpendicular, or at various angles to the lumen, with junctional membranes often dipping into the lumen or CNS parenchyma (Fig. 3A, c, B, c, and D). The polarized expression of Glut1 at the abluminal membrane was not affected (Supplementary Fig. 9).

To determine whether junctional abnormalities are due to a lack of pericytes, or other defects in *Pdgfrb*$^{-/-}$ mice, we analysed the function, expression and localization of tight-junction proteins in purified brain endothelial cells cultured alone or with a feeding layer of purified brain pericytes. Purified CNS endothelial cells expressed the tight-junction proteins occludin and claudin 5, which were localized to cellular borders (Fig. 3G, H). Notably, endothelial cells cultured alone often contained large gaps between cell connections, whereas the endothelial

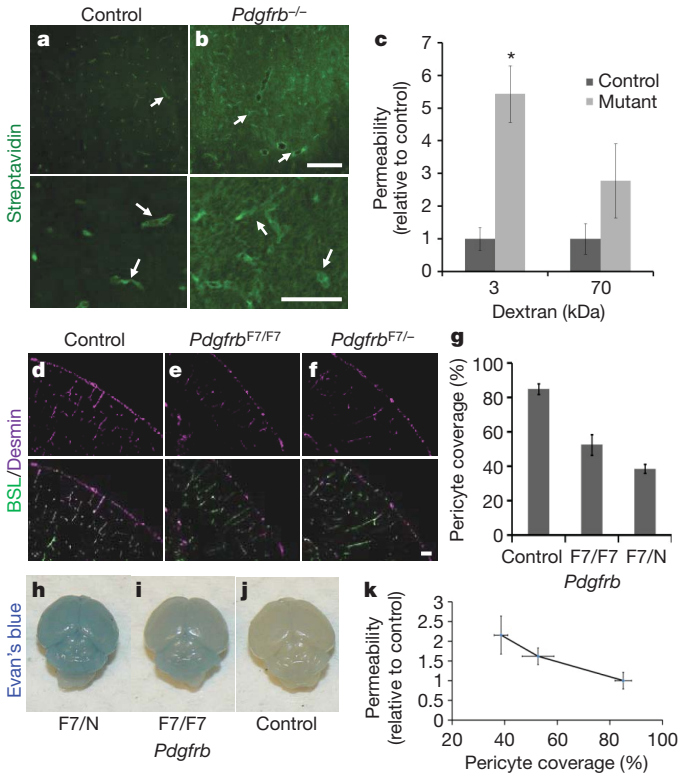

Figure 2 | Pericytes are required for BBB formation. **a**, **b**, E18 *Pdgfrb*$^{-/-}$ mice (**b**) and littermate controls (**a**) were given a trans-cardiac perfusion of biotin, and tissue sections were stained with streptavidin (green; white arrows indicate tracer in vessels). Scale bars represent 200 μm (upper panel) and 100 μm (lower panel). **c**, E18 *Pdgfrb*$^{-/-}$ mice and littermate controls were given a trans-cardiac perfusion of 3 kDa or 70 kDa biotinylated dextran, tissue sections stained with streptavidin-Alexa 488, fluorescence was quantified in ImageJ and permeability relative to control was graphed. *$P < 0.05$ by Student's *t*-test. **d**–**f**, Neonatal mouse cerebral cortex from *Pdgfrb*$^{F7/-}$ (**f**), *Pdgfrb*$^{F7/F7}$ (**e**) and littermate controls (**d**) were stained with BSL (green, **d**–**f** (bottom)) and for pericytes with anti-desmin (purple, **d**–**f**). Scale bar represents 100 μm. **g**, Pericyte coverage of CNS vessels in *Pdgfrb*$^{F7/-}$, *Pdgfrb*$^{F7/F7}$ and littermate control mice was quantified by analysing per cent length of BSL^{+} vessels opposed to desmin^{+} pericytes. **h**–**j**, P5 *Pdgfrb*$^{F7/-}$ mice (**h**), *Pdgfrb*$^{F7/F7}$ mice (**i**) and littermate controls (**j**) were given an intraperitoneal injection of Evan's blue dye, and their brains were dissected the following day after PBS perfusion. **k**, Neonatal *Pdgfrb*$^{F7/-}$, *Pdgfrb*$^{F7/F7}$ and littermate controls were given a trans-cardiac perfusion of biotin and leakage was quantified in tissue sections with streptavidin-Alexa-488 (*y* axis) and graphed versus pericyte coverage (*x* axis; values from panel **g**). All error bars represent s.e.m.

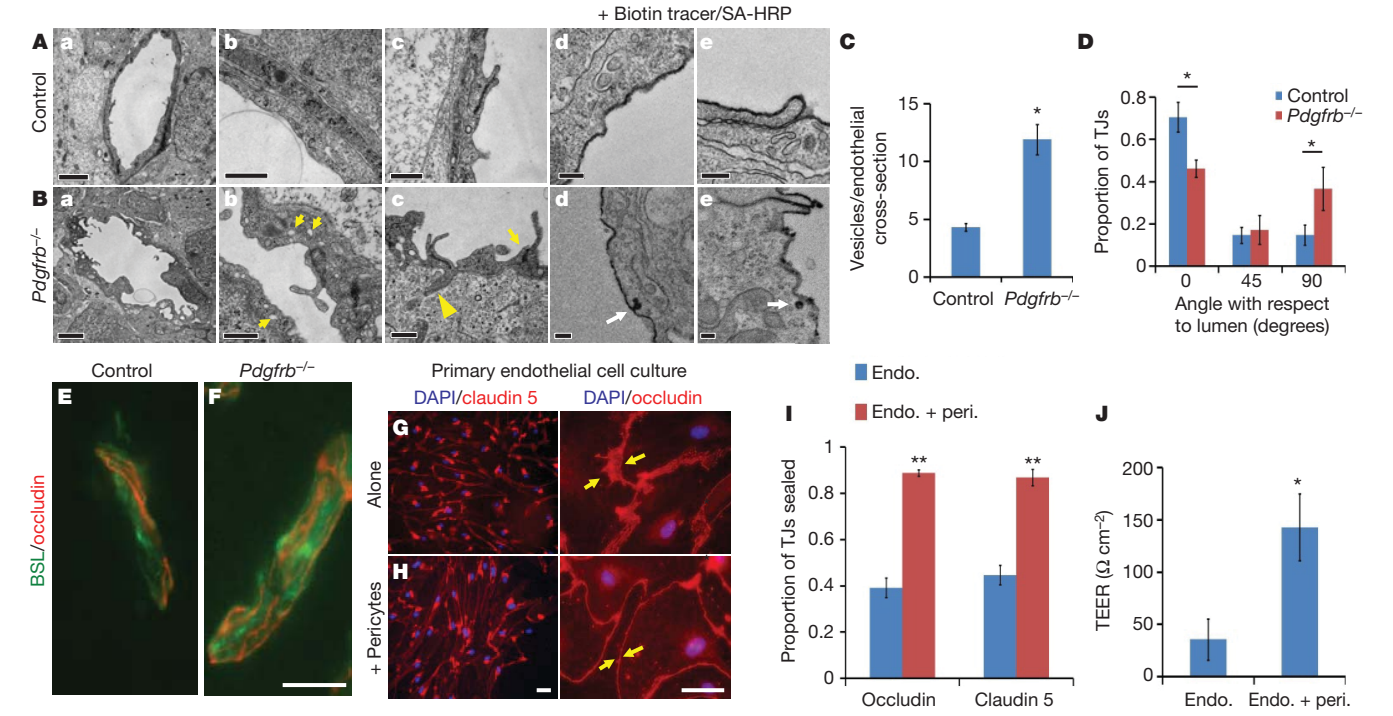

Figure 3 | Pericytes regulate structural aspects of the BBB. **A**, **B**, Electron microscopy images of CNS vessels from E18 *Pdgfrb*$^{-/-}$ mice (**B**) and littermate controls (**A**) including whole endothelial cell cross-sections (**a**), cytoplasm (**b**; yellow arrows indicate cytoplasmic vessels), tight junctions (**c**; yellow arrows indicate altered junction alignment; yellow arrowheads indicate junctions dipping into parenchyma), and after perfusion with biotin followed by staining with streptavidin–HRP (**d**, **e**; white arrows indicate uptake of tracer). Scale bars represent 2 μm (**a**), 0.5 μm (**b**, **c**) and 0.2 μm (**d**, **e**). **C**, Quantification of the number of vesicles per endothelial cross-section for *Pdgfrb*$^{-/-}$ mice and littermates. **D**, Angles of tight junctions (TJs) for *Pdgfrb*$^{-/-}$ mice and littermate controls were classified as parallel to the lumen (0°), perpendicular to the lumen (90°) or in between (45°). *$P < 0.05$ by Student's *t*-test. **E**, **F**, Cerebral cortex of E18 *Pdgfrb*$^{-/-}$ mice (**F**) and littermate controls (**E**) were stained with BSL (green) and anti-occludin (red). Scale bars represent 20 μm. **G**, **H**, Purified murine brain endothelial cells were cultured alone (**G**) or with a feeding layer of purified brain pericytes (**H**) and stained with DAPI (blue) and anti-claudin 5 (left, red) or anti-occludin (right, red; yellow arrows indicate cell borders). Scale bars represent 100 μm (left) and 50 μm (right). **I**, Per cent length of sealed claudin 5 and occludin junctions in endothelial cells cultured alone or with pericyte feeder layers. **$P < 0.01$ by Student's *t*-test. **J**, TEER measurements for purified murine brain endothelial cells cultured alone or with a feeding layer of purified brain pericytes. *$P < 0.05$ by Student's *t*-test. All error bars represent s.e.m.

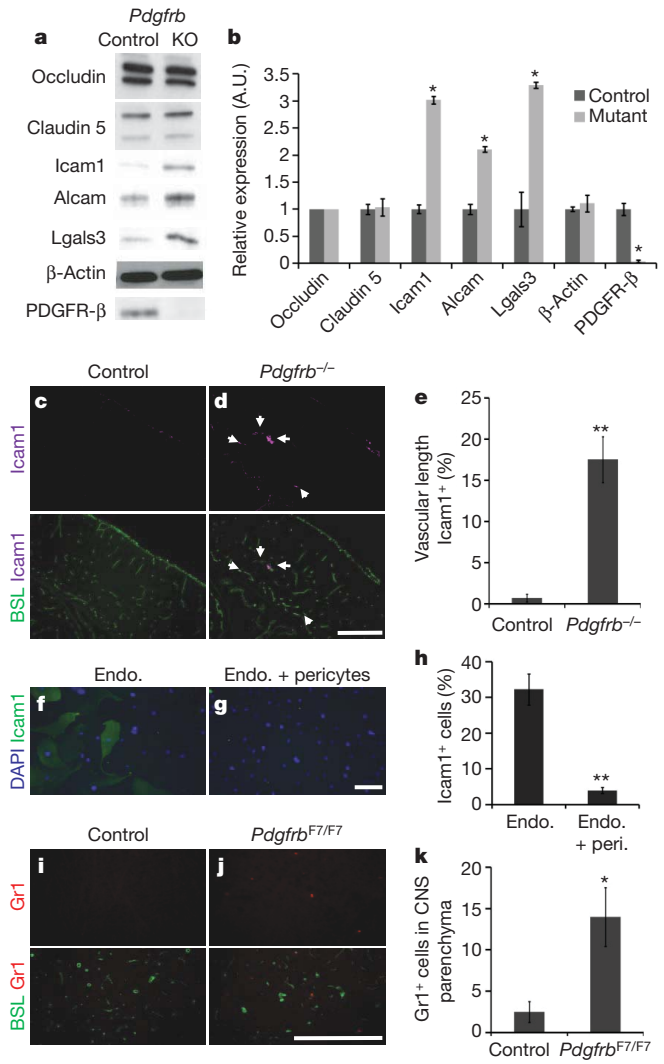

Figure 4 | Vascular expression of LAMs in *Pdgfrb*$^{-/-}$ mice. **a**, **b**, Western blots of brain lysates from E18 *Pdgfrb*$^{-/-}$ (KO) and littermate controls, probing occludin, claudin 5, Icam1, Alcam, Lgals3, β-actin and PDGFR-β. **a**, Representative blots; **b**, quantification; $*P < 0.05$ by Student's *t*-test. **c**–**e**, Cerebral cortex of E18 *Pdgfrb*$^{-/-}$ mice (**d**) and littermate controls (**c**) were stained with anti-Icam1 (purple) and BSL (green, bottom; white arrows indicate Icam1$^+$ vessels), and per cent Icam1$^+$ vascular length was quantified (**e**). Scale bar represents 250 μm. $**P < 0.005$ by Student *t*-test. **f**–**h**, Purified murine brain endothelial cells cultured alone (**f**) or with a feeding layer of purified brain pericytes (**g**) and stained for DAPI (blue) and anti-Icam1 (green), and proportion of Icam1$^+$ cells was quantified (**h**). Scale bar represents 200 μm. $**P < 0.005$ by Student *t*-test. **i**–**k**, Five-week-old *Pdgfrb*$^{F7/F7}$ mice (**j**) and littermate controls (**i**) were stained with anti-Gr1 (red) and BSL (green, bottom), and number of Gr1$^+$ cells per sagittal section was counted (**k**). Scale bar represents 250 μm. $*P < 0.05$ by Students *t*-test. All error bars represent s.e.m.

junctions sealed and the intercellular space diminished when they were cultured with pericytes (Fig. 3G–I). This was accompanied by a four-fold increase in trans-endothelial cell electrical resistance (TEER), demonstrating that endothelial tight junctions are functionally tighter in the presence of pericytes (Fig. 3J).

To determine whether pericytes regulate endothelial gene expression, we used microarray analysis to compare the gene expression of CD31$^+$ vascular cells purified from *Pdgfrb*$^{-/-}$ mice and littermate controls. In *Pdgfrb*$^{-/-}$ mice, no downregulation of BBB genes was observed, including tight-junction proteins and transporters (Supplementary Table 1 and Fig. 4a, b). Thus, pericytes are not necessary for induction of BBB-specific genes. In the absence of pericytes, however, expression of genes known to increase vascular permeability, including *Angpt2*, *Plvap* and leukocyte adhesion molecules (LAMs), were upregulated. In *Pdgfrb*$^{-/-}$ mice we observed a loss of vascular *Angpt1*, a Tie2 receptor ligand that decreases permeability, and a corresponding increase in *Angpt2*, a Tie2 ligand that increases vascular permeability[18,19] (Supplementary Table 1), and co-culture of a feeder layer of pericytes with CNS endothelial cells was sufficient to decrease endothelial Angpt2 expression (Supplementary Fig. 12). *Pdgfrb*$^{-/-}$ mice also exhibited an increase in endothelial *Plvap* expression (Supplementary Table 1), which was verified by immunofluorescence (Supplementary Fig. 10). Plvap is involved in endothelial vesicle trafficking, and is highly expressed in permeable peripheral vessels and is upregulated in CNS endothelial cells during pathological breakdown of the BBB[20,21]. Therefore, pericytes may limit transcytosis by suppressing Plvap.

We further examined the gene expression of acutely purified pericytes to identify pericyte-secreted signals (Supplementary Table 2). We identified that pericytes express molecules that regulate BBB properties including *Angpt1* and *Ace2* (refs 12, 22), as well as a number of other signalling molecules and matrix components. Furthermore, the extracellular matrix is altered in the *Pdgfrb*$^{-/-}$ mouse, including a decrease in several collagen subunits and an upregulation of MMP9, a protease that increases the permeability of the BBB during disease (Supplementary Fig. 11)[23,24].

The transcription of several LAMs, including *Icam1*, *Alcam* and *Lgals3*, were significantly upregulated in the vasculature of *Pdgfrb*$^{-/-}$ mice (Supplementary Table 1), and we confirmed a corresponding increase in protein expression (Fig. 4a, b). We found that Icam1 was robustly upregulated in specific segments of the vasculature in *Pdgfrb*$^{-/-}$ mice (Fig. 4c–e), and further demonstrated that co-culture of pericytes with endothelial cells is sufficient to decrease the number of Icam1$^+$ endothelial cells (Fig. 4f–h). These data indicate that pericytes may provide signals that limit CNS immune surveillance, a critical feature of the BBB. Indeed, we observed an increase in the number of Gr1$^+$ leukocytes in the CNS parenchyma of pericyte-deficient mice (Fig. 4i–k).

These findings demonstrate that pericytes are required for BBB formation during development, and absolute pericyte coverage controls relative BBB permeability. Although astrocytes are not required to initially induce the BBB, it remains likely that astrocytes act to regulate the maintenance of the BBB and its response to neural function and disease. In fact, reactive astrocytes are necessary for BBB repair after injury[25]. Interestingly, even in the absence of pericytes, embryonic CNS endothelial cells express many BBB-specific molecules, indicating that neural progenitors may induce BBB gene expression. Indeed, neural-progenitor-derived Wnts are critical for CNS angiogenesis and the induction of BBB-specific transporter expression[26–28]. We propose a new model for BBB formation: endothelial cells are induced to express BBB-specific genes by interactions with neural progenitors, and then the functional integrity of the BBB is regulated by pericytes during development and astrocytes in adulthood (Supplementary Fig. 13).

These findings have important implications for understanding BBB breakdown and repair, which is a common component of many neurodegenerative disorders, stroke, brain tumours, CNS trauma, multiple sclerosis and diabetic retinopathy[1]. Notably, loss of pericytes occurs at early stages of diabetic retinopathy, and thus probably has a role in the vascular permeability defects observed during this disease[29]. The finding that pericytes are necessary for limiting CNS immune surveillance has implications for controlling neuroinflammation. For instance, pericytes inhibit the expression of Alcam, which is upregulated in CNS vessels in multiple sclerosis (MS) patients and enhances leukocyte migration across endothelial cells[30]. Identification of molecular mechanisms by which pericytes regulate BBB integrity may lead to new treatments for these diseases.

METHODS SUMMARY

Immunohistochemistry. Rodent tissues were fixed with 4% paraformaldehyde, 10% trichloroacetic acid or 95% ethanol followed by acetone. Tissue sections were blocked with 50% goat serum, permeabilized with 0.2% Triton X-100, and stained

with appropriate primary and secondary antibodies. Slides were mounted in vectashield with DAPI (Vector Labs) and visualized by fluorescence microscopy.

BBB permeability assays. Anaesthetized rodents were given a trans-cardiac perfusion, with a Dynamax peristaltic pump, of DPBS (Gibco) containing EZ-link sulfo NHS Biotin (Pierce) or biotinylated fixable dextrans (Invitrogen), followed by 4% paraformaldehyde. Tissue cryosections were stained with streptavidin Alexa-488 (Invitrogen) and analysed by fluorescence microscopy.

Cell culture. CNS endothelial cells were purified by anti-CD31 immunopanning and CNS pericytes were purified by anti-PDGFR-β immunopanning. For immunofluorescence analysis, CNS endothelial cells were grown on coverslips alone, or with a feeder layer of CNS pericytes grown on cell culture inserts. For TEER measurements, CNS endothelial cells were grown on cell culture inserts alone, or with a pericyte feeder layer grown in the culture well bottom beneath, and resistance measurements were recorded with an EVOM voltmeter.

Electron microscopy. E18 *Pdgfrb*$^{-/-}$ and littermate controls were fixed in 2% glutaraldehyde/4% paraformaldehyde, and processed for electron microscopy. To image tracer permeability, E18 *Pdgfrb*$^{-/-}$ and littermate controls were given a trans-cardiac perfusion of DPBS (Gibco) containing EZ-link sulfo NHS Biotin (Pierce) followed by 4% paraformaldehyde, and frozen tissue sections were fixed with 2% glutaraldehyde/4% paraformaldehyde then stained with a HRP-tagged streptavidin (Invitrogen) followed by DAB reaction.

Full Methods and any associated references are available in the online version of the paper at www.nature.com/nature.

Received 14 April 2009; accepted 23 September 2010.
Published online 13 October 2010.

1. Zlokovic, B. V. The blood-brain barrier in health and chronic neurodegenerative disorders. *Neuron* **57,** 178–201 (2008).
2. Stewart, P. A. & Wiley, M. J. Developing nervous tissue induces formation of blood-brain barrier characteristics in invading endothelial cells: a study using quail–chick transplantation chimeras. *Dev. Biol.* **84,** 183–192 (1981).
3. Janzer, R. C. & Raff, M. C. Astrocytes induce blood-brain barrier properties in endothelial cells. *Nature* **325,** 253–257 (1987).
4. Bauer, H. C. *et al.* Neovascularization and the appearance of morphological characteristics of the blood-brain barrier in the embryonic mouse central nervous system. *Brain Res. Dev. Brain Res.* **75,** 269–278 (1993).
5. Bolz, S., Farrell, C. L., Dietz, K. & Wolburg, H. Subcellular distribution of glucose transporter (GLUT-1) during development of the blood-brain barrier in rats. *Cell Tissue Res.* **284,** 355–365 (1996).
6. Butt, A. M., Jones, H. C. & Abbott, N. J. Electrical resistance across the blood-brain barrier in anaesthetized rats: a developmental study. *J. Physiol. (Lond.)* **429,** 47–62 (1990).
7. Ek, C. J., Dziegielewska, K. M., Stolp, H. & Saunders, N. R. Functional effectiveness of the blood-brain barrier to small water-soluble molecules in developing and adult opossum (Monodelphis domestica). *J. Comp. Neurol.* **496,** 13–26 (2006).
8. Hirase, T. *et al.* Occludin as a possible determinant of tight junction permeability in endothelial cells. *J. Cell Sci.* **110,** 1603–1613 (1997).
9. Kniesel, U., Risau, W. & Wolburg, H. Development of blood-brain barrier tight junctions in the rat cortex. *Brain Res. Dev. Brain Res.* **96,** 229–240 (1996).
10. Korn, J., Christ, B. & Kurz, H. Neuroectodermal origin of brain pericytes and vascular smooth muscle cells. *J. Comp. Neurol.* **442,** 78–88 (2002).
11. Dohgu, S. *et al.* Brain pericytes contribute to the induction and up-regulation of blood-brain barrier functions through transforming growth factor-β production. *Brain Res.* **1038,** 208–215 (2005).
12. Hori, S., Ohtsuki, S., Hosoya, K., Nakashima, E. & Terasaki, T. A pericyte-derived angiopoietin-1 multimeric complex induces occludin gene expression in brain capillary endothelial cells through Tie-2 activation *in vitro*. *J. Neurochem.* **89,** 503–513 (2004).
13. Lai, C. H. & Kuo, K. H. The critical component to establish *in vitro* BBB model: Pericyte. *Brain Res. Brain Res. Rev.* **50,** 258–265 (2005).
14. Lindahl, P., Johansson, B. R., Leveen, P. & Betsholtz, C. Pericyte loss and microaneurysm formation in PDGF-B-deficient mice. *Science* **277,** 242–245 (1997).
15. Tallquist, M. D., French, W. J. & Soriano, P. Additive effects of PDGF receptor β signaling pathways in vascular smooth muscle cell development. *PLoS Biol.* **1,** e52 (2003).
16. Hellstrom, M. *et al.* Lack of pericytes leads to endothelial hyperplasia and abnormal vascular morphogenesis. *J. Cell Biol.* **153,** 543–554 (2001).
17. Shepro, D. & Morel, N. M. Pericyte physiology. *FASEB J.* **7,** 1031–1038 (1993).
18. Lee, S. W., Kim, W. J., Jun, H. O., Choi, Y. K. & Kim, K. W. Angiopoietin-1 reduces vascular endothelial growth factor-induced brain endothelial permeability via upregulation of ZO-2. *Int. J. Mol. Med.* **23,** 279–284 (2009).
19. Nag, S., Papneja, T., Venugopalan, R. & Stewart, D. J. Increased angiopoietin2 expression is associated with endothelial apoptosis and blood-brain barrier breakdown. *Lab. Invest.* **85,** 1189–1198 (2005).
20. Shue, E. H. *et al.* Plasmalemmal vesicle associated protein-1 (PV-1) is a marker of blood-brain barrier disruption in rodent models. *BMC Neurosci.* **9,** 29 (2008).
21. Ioannidou, S. *et al.* An *in vitro* assay reveals a role for the diaphragm protein PV-1 in endothelial fenestra morphogenesis. *Proc. Natl Acad. Sci. USA* **103,** 16770–16775 (2006).
22. Wosik, K. *et al.* Angiotensin II controls occludin function and is required for blood brain barrier maintenance: relevance to multiple sclerosis. *J. Neurosci.* **27,** 9032–9042 (2007).
23. Gidday, J. M. *et al.* Leukocyte-derived matrix metalloproteinase-9 mediates blood-brain barrier breakdown and is proinflammatory after transient focal cerebral ischemia. *Am. J. Physiol. Heart Circ. Physiol.* **289,** H558–H568 (2005).
24. He, Z. J., Huang, Z. T., Chen, X. T. & Zou, Z. J. Effects of matrix metalloproteinase 9 inhibition on the blood brain barrier and inflammation in rats following cardiopulmonary resuscitation. *Chin. Med. J. (Engl.)* **122,** 2346–2351 (2009).
25. Bush, T. G. *et al.* Leukocyte infiltration, neuronal degeneration, and neurite outgrowth after ablation of scar-forming, reactive astrocytes in adult transgenic mice. *Neuron* **23,** 297–308 (1999).
26. Weidenfeller, C., Svendsen, C. N. & Shusta, E. V. Differentiating embryonic neural progenitor cells induce blood-brain barrier properties. *J. Neurochem.* **101,** 555–565 (2007).
27. Daneman, R. *et al.* Wnt/β-catenin signaling is required for CNS, but not non-CNS, angiogenesis. *Proc. Natl Acad. Sci. USA* **106,** 641–646 (2009).
28. Stenman, J. M. *et al.* Canonical Wnt signaling regulates organ-specific assembly and differentiation of CNS vasculature. *Science* **322,** 1247–1250 (2008).
29. Motiejunaite, R. & Kazlauskas, A. Pericytes and ocular diseases. *Exp. Eye Res.* **86,** 171–177 (2008).
30. Cayrol, R. *et al.* Activated leukocyte cell adhesion molecule promotes leukocyte trafficking into the central nervous system. *Nature Immunol.* **9,** 137–145 (2008).

Supplementary Information is linked to the online version of the paper at www.nature.com/nature.

Acknowledgements We thank J. Perrino for electron microscopy preparations. Work was supported by grants from the NINDS (R01-NS045621; B.A.B), Myelin Repair Foundation (B.A.B., R.D.), NMSS (Grant-RG3936A7; B.A.B.), UCSF Fellow's Program (R.D.) and AHA (R.D.).

Author Contributions R.D. and B.A.B. designed experiments and wrote the manuscript. R.D., L.Z. and A.A.K. performed and analysed experiments.

Author Information Reprints and permissions information is available at www.nature.com/reprints. The authors declare no competing financial interests. Readers are welcome to comment on the online version of this article at www.nature.com/nature. Correspondence and requests for materials should be addressed to R.D. (Richard.daneman@ucsf.edu).

METHODS

Animals. Sprague–Dawley rats and C57BL/6 mice were obtained from Charles River. Mice harbouring *Pdgfrb*$^{-}$ and *Pdgfrb*^{F7} alleles were obtained from Phillippe Soriano (Fred Hutchinson Cancer Research Center), and lines were maintained by breeding with C57BL/6 mice.

Immunohistochemistry. For time course experiments, whole rat and mouse embryos before E15, and dissected brains of embryos between E15 and birth, were fixed overnight in 4% paraformaldehyde at 4 °C. Postnatal rats and mice were anaesthetized with a ketamine (100 mg kg^{-1})/xylazine (20 mg kg^{-1}) cocktail, and perfused with PBS followed by 4% paraformaldehyde with a dynamax peristaltic pump and then dissected brains were fixed overnight in 4% paraformaldehyde at 4 °C. Staining was performed as described previously[27], with antibodies directed against PDGFR-β (R&D systems, eBiosciences) and Ng2 (Chemicon) for pericytes, PDGFR-α for OPCs (Abcam), Aqp4 for astrocytes (sigma), Glut1 (Chemicon), Pgp (Sigma) and Icam1 (Abcam), and with appropriate Alexa-conjugated secondary antibodies and counter-stained with BSL-fluorescein (Vector Labs). For ZO-1 and Plvap immunofluoresence, embryos were fixed with 10% trichloroacetic acid for 1 h on ice, before cryopreservation and staining with anti-ZO-1 antibody (Invitrogen) or anti-Plvap antibody (AbD Serotec). Staining for occludin and claudin 5 was achieved by flash freezing dissected brains, or whole embryos for ages less than E15, in OCT. Tissue cryosections were obtained and fixed in cold 95% ethanol for 30 min, followed by 1 min in room temperature acetone. Sections were then rehydrated in PBS, blocked in 50% goat serum and stained with antibodies directed against occludin (Invitrogen), and claudin 5 (Invitrogen), followed by appropriate Alexa-fluorophore-conjugated secondary antibodies and counterstained with BSL-fluorescein (Vector Labs). Slides were mounted in vectashield with DAPI (Vector Labs) and visualized by fluorescence microscopy.

For pericyte-deficient mice, *Pdgfrb*$^{-/-}$ and littermate control embryos were flash-frozen and stained using the ethanol/acetone fixation described above with antibodies directed against occludin (Invitrogen), claudin 5 (Invitrogen) and Plvap (AbD Serotec). For Icam1, Ng2 and Glut1 staining, brains of dissected *Pdgfrb*$^{-/-}$ and littermate control embryos were fixed overnight in 4% paraformaldehyde at 4 °C and stained as described previously, with antibodies directed against Icam1 (Abcam), Ng2 (Chemicon) or Glut1 (Chemicon). For Gr1 staining, 5-week-old *Pdgfrb*$^{F7/F7}$ and littermate controls were perfusion fixed, and dissected brains were further fixed overnight in 4% paraformaldehyde at 4 °C and stained as described previously, with antibodies directed against Gr1 (gift from I. Weismann). For comparisons of *Pdgfrb*$^{-/-}$ and littermate control brains, sections were analysed on a Nikon Eclipse E800 microscope and images were taken with a Diagnostics Instrument SPOT camera with set exposure to appropriately compare staining between genotypes. Percent length of vasculature with intense Icam1 staining was measured using ImageJ ($n \geq 4$ each for mutant and littermate controls for each stain). For pericyte staining comparing *Pdgfrb*$^{+/+}$, *Pdgfrb*$^{+/-}$ and *Pdgfrb*$^{-/-}$ mice, tissue sections were stained with anti-Zic1 (Novus) and anti-desmin antibody (Dako) after antigen retrieval by steaming in a 10 mM citrate buffer for 30 min, or anti-NG2 (Chemicon). For quantification of pericyte number in *Pdgfrb*$^{+/+}$ and *Pdgfrb*$^{+/-}$ mice the number of Zic^{+} nuclei was counted and divided by vascular length quantified in ImageJ ($n \geq 7$ for each genotype). Pericyte coverage was quantified using ImageJ to measure the length of BSL^{+} vessels associated with desmin^{+} pericyte processes ($n \geq 5$ for each genotype). Total Gr1^{+} cells outside BSL^{+} vessels per medial sagittal brain section were counted ($n = 4$ each for *Pdgfrb*$^{F7/F7}$ and littermate controls). For desmin staining, neonatal *Pdgfrb*$^{F7/N}$, *Pdgfrb*$^{F7/F7}$ and littermate controls were perfusion-fixed and stained with anti-desmin antibody (Dako) after antigen retrieval by steaming in a 10 mM citrate buffer for 30 min. Pericyte coverage was quantified using ImageJ to measure the length of BSL^{+} vessels associated with desmin^{+} pericyte processes ($n \geq 3$ for each genotype). All quantification was performed blind to genotype.

BBB permeability assays. Animals were anaesthetized with a ketamine (100 mg kg^{-1})/xylazine (20 mg kg^{-1}) cocktail, and then the thoracic cavity was opened to reveal the heart. The right ventricle was severed and then a DPBS (Gibco) solution containing 1 mg ml^{-1} EZ-link sulfo NHS-biotin (Pierce) was perfused into the left ventricle using a Dynamax peristaltic pump for 3 min, followed by 5 min of perfusion with 4% paraformaldehyde. The flow rate of the pump was adjusted to match the cardiac output of the rats or mice. Tissues, including the brain, liver and muscle, were dissected and further submersion fixed in 4% paraformaldehyde overnight at 4 °C, before being submerged in 30% sucrose. Ten micrometre cryosections were generated after the tissue was frozen in a 2:1 30% sucrose: OCT mixture. For E15 time points, the entire embryo was submersion-fixed and processed. Tissue sections were treated with a 50% goat serum blocking solution, before staining with streptavidin-Alexa 488 (Invitrogen). Staining of streptavidin was analysed with a Nikon Eclipse E800 microscope and images were taken with a Diagnostics Instrument SPOT camera and analysed by SPOT software. For comparisons of *Pdgfrb*$^{-/-}$ and littermate control brains, pregnant mice were anaesthetized with ketamine/xylazine, and embryos were extracted and chosen blind to genotype for perfusions. Six embryos were chosen from each litter, one as a control perfused without tracer. The perfusion setup was standardized to minimize fluctuations for pH (7.09 ± 0.005 s.d.) and pO_2 (136.1 mm Hg ± 2.0 s.d.) and the perfusion pressure was maintained digitally with the dynamax pump. The heart beat was monitored and all embryos maintained heart beat throughout tracer perfusions. Perfusions were performed with EZ-link sulfo NHS-biotin (0.5 mg ml^{-1}, Pierce), 3 kDa biotinylated fixable dextran (0.15 mg ml^{-1}, Invitrogen) or 70 kDa biotinylated fixable dextran (3.5 mg ml^{-1} Invitrogen), and micrographs were taken with set exposure to appropriately compare the amount of biotin in the brain tissue. The concentrations of the dextrans were matched for molar concentrations ($n \geq 6$ for each sample group for each tracer). Fluorescence in tissue sections was compared by ImageJ software, using tissue sections of embryos perfused with DPBS without tracer as a background control. *Pdgfrb*$^{+/+}$ and *Pdgfrb*$^{+/-}$ mice were combined as littermate controls, as we did not observe any difference in leakage between the two genotypes. For Evan's blue extravasation assays, P5 *Pdgfrb*$^{F7/-}$, *Pdgfrb*$^{F7/F7}$ and littermate controls were given an intraperitoneal injection of 10 µl 2% Evan's blue. After 1 day, animals were perfused as described above with PBS followed by paraformaldehyde. Dissected brains were photographed. For quantification of biotin leakage in neonatal *Pdgfrb*$^{+/+}$ and *Pdgfrb*$^{+/-}$ mice, and in neonatal *Pdgfrb*$^{F7/-}$, *Pdgfrb*$^{F7/F7}$ and littermate controls, trans-cardiac perfusion of biotin tracer was performed, followed by staining of tissue sections with streptavidin, and quantification of leakage with ImageJ. In each case, perfusions and analysis was done blind to genotype.

Electron microscopy. Cerebral cortex from E18 *Pdgfrb*$^{-/-}$ and littermate controls was fixed in 2% glutaraldehyde/4% paraformaldehyde in sodium cacodylate buffer overnight at 4 °C and processed for electron microscopy as described previously[31] ($n = 3$ for both mutant and littermate controls). To visualize tracer permeability by electron microscopy, E18 *Pdgfrb*$^{-/-}$ and littermate controls were perfused with biotin followed by paraformaldehyde as described above. Frozen tissue sections were fixed with 2% glutaraldehyde/4% paraformaldehyde in sodium cacodylate buffer overnight and stained with a HRP-tagged streptavidin (Invitrogen) followed by DAB reaction before being processed for electron microscopy.

Endothelial cell culture. Endothelial cells from adult C57BL/6 mice brains were purified and cultured as previously described[27] and grown with puromycin for the first 3 days. For mouse and rat brain pericytes, brain tissue suspensions were prepared as described previously[27], and cell suspensions were incubated on two dishes coated with an anti-CD45 antibody to deplete microglia cells, followed by a dish coated with anti-PDGFR-β to select pericytes. The pericytes were recovered by trypsin treatment and plated on PDL-coated cell culture filter inserts in a DMEM-based medium (Invitrogen) containing SATO, insulin, pyruvate, penicillin, streptomycin, glutamine and 10% fetal calf serum (Invitrogen). After 2.5 weeks, pericyte growth media was exchanged for endothelial growth media, and pericyte inserts were added to endothelial cells for 3 days. Endothelial cells were fixed with 4% paraformaldehyde for 10 min, then block/permeabilized for 30 min in 50% goat serum and 0.2% Triton X-100, and stained with primary antibodies directed against occludin (Invitrogen), claudin 5 (Invitrogen), Icam1 (Abcam) or Angpt2 (Abcam) and appropriate Alexa-fluorophore-conjugated secondary antibodies, mounted in vectashield with DAPI and images were taken with a Diagnostics Instrument SPOT camera analysed using a Nikon Eclipse E800 microscope. Per cent vascular length with closed tight junctions was analysed using ImageJ software. Specifically, total length of cell junctions between two cells was measured, and then the length of these junctions where a single band of occludin or claudin 5 (sealed-staining between arrows in Fig. 3H, right panel) or two bands with diffuse staining between (unsealed-staining between arrows in Fig. 3G, right panel) was measured ($n \geq 3$ paired cultures of endothelial cells alone and endothelial cells with pericyte feeder layer for each marker). For TEER measurements, endothelial cells were isolated as described and grown on the filter membrane of Costar HTS transwell plates, and cultured in puromycin for 3 days, before being transferred to a new dish with media containing hydrocortisone, without puromycin. In the new dish, half the filter membranes were placed in wells with pericytes cultured on the bottom well. Resistance measurements were taken between 10–19 days after co-culture with an EVOM voltmeter (World Precision Instruments) and subtracted from resistance of membrane without cellular culture. Unit resistance was calculated by multiplying the resistance by the area of the filter membrane, and averaged for each sample ($n = 6$ paired cultures of endothelial cells alone and endothelial cells with pericyte feeder layer).

GeneChip. Vascular cells from E18 *Pdgfrb*$^{-/-}$ and littermate controls were purified based on methods described previously[27]. Acutely purified pericytes were purified from mouse brain by anti-PDGFR-β immunopanning as described. Purification of RNA from acutely isolated cells, generation of biotinylated cRNA, subsequent hybridization to Affymetrix Mouse Genome 430 2.0 Arrays

and raw image analysis with Affymetrix GCOS 1.3 software was performed as previously described[32].

Western blots. Cerebral cortex from E18 *Pdgfrb*$^{-/-}$ and littermate controls were homogenized and re-suspended and lysed in RIPA buffer (50 mM Tris pH 7.4, 150 mM NaCl, 1 mM EDTA, 1% Triton X-100, 0.1% SDS), and protein concentration was quantified using BCA protein assay (Pierce). Samples were analysed by SDS–PAGE as previously described[33]. Briefly, samples were resolved on SDS–PAGE and transferred to PVDF membranes. Membranes were blocked with 5% milk solution and then incubated with antibodies directed against occludin (Invitrogen), claudin 5 (Invitrogen), Icam1 (Abcam), Alcam (R & D Systems), Lgals3 (R & D Systems), Col I (Abcam), Col III (Abcam), vitronectin (Abcam), MMP9 (Abcam), PDGFR-β (eBiosciences) or β-actin (Sigma) followed by incubation with an appropriate secondary conjugated to HRP (Jackson 1:10,000) and visualized using a chemiluminescent ECL substrate for HRP (GE), and either exposed on film and quantified with ImageJ or imaged with a Fuji-Film LAS 4000 and analysed with Multi Gauge V3.0 software ($n = 2$–5 for mutant and $n = 4$–8 for littermate controls).

31. Watkins, T. A., Emery, B., Mulinyawe, S. & Barres, B. A. Distinct stages of myelination regulated by γ-secretase and astrocytes in a rapidly myelinating CNS coculture system. *Neuron* **60,** 555–569 (2008).
32. Cahoy, J. D. *et al.* A transcriptome database for astrocytes, neurons, and oligodendrocytes: a new resource for understanding brain development and function. *J. Neurosci.* **28,** 264–278 (2008).
33. Chan, J. R. *et al.* NGF controls axonal receptivity to myelination by Schwann cells or oligodendrocytes. *Neuron* **43,** 183–191 (2004).